Journal of Env. Geogr. Vol. III. No. 1-4. pp. 31-40

CREATING EXCESS WATER INUNDATION MAPS BY SUB-PIXEL CLASSIFICATION OF MEDIUM RESOLUTION SATELLITE IMAGES

Mucsi, L.[1] **– Henits, L.**[1]

[1]Department of Physical Geography and Geoinformatics, University of Szeged, Hungary

Abstract

Excess water frequency factor, which indicates the number of inundations in the area under study within a certain period of time, is the most dynamic variable among the parameters applied in the complex methodology of excess water hazard mapping. Creating excess water inundation maps, representing the situation in the most realistic way, was hitherto a critical moment in excess water hazard mapping. Instead of field measurements, since the database of Landsat satellite images became accessible in 2009, it is possible to process satellite images taken from the year 1985, with using new, non-traditional methods different from the pixel-based classification. These methods are mainly sub-pixel based classifications and they are applied principally on images taken in periods of extended excess water inundation, under clear weather conditions. In our research project, medium-scale mapping was supported principally by hand-held or mounted multispectral (the bands of visible and infrared light) digital aerial photography. The photo-taking process, depending on the actual meteorological conditions, can be flexibly accomplished in the most extended inundation period, thus it is possible to create excess water maps at the scale of 1:10000.

INTRODUCTION

Excess water frequency factor, which indicates the number of inundations in the area under study within a certain period of time, is the most dynamic variable among the parameters applied in the complex methodology of excess water hazard mapping (Pálfai et al., 2004). Creating excess water inundation maps, representing the situation in the most realistic way, was hitherto a critical moment in excess water hazard mapping, since the creation of an excess water map via traditional methods and field survey is time-consuming and contains several possibilities for committing errors (Licskó B., 2009). One of the major problems regarding field mapping is that the determination of the shape of an extended excess water area is uncertain from a close-to-surface point, owing to the low angle of vision. It is also difficult to determine the extension of the patches by walking round their boundary using kinematic GPS. This method gives particularly indefinite results, because there is a continuous transition between the open water surface, the slightly saturated soil and the dry soil, therefore their classification is problematic.

While mapping excess water inundation, efforts should be made to cover a large area, and to create large-scale thematic maps in a cost effective way. This way, not only the open water surfaces, but also the transitional areas could be mapped. Large-scale mapping is supported principally by hand-held or mounted multispectral (the bands of visible and infrared light) digital aerial photography. The photo-taking process, depending on the actual meteorological conditions, can be flexibly accomplished in the most extended inundation period, thus it is possible to create excess water maps at the scale of 1:10000 (Licskó B., 2009). However, the survey of vast areas is expensive and requires considerable post-processing.

The mapping of excess water inundation is more economical if the inundation map derives from remote sensing data covering vast areas. Excess water inundation maps based on satellite images have been created by the Institute of Geodesy, Cartography and Remote Sensing (FÖMI) since 1998. A significant number of maps were created in the years 1999 and 2000, when the inundation was very extended (Csornai G. et al., 2000). By means of 0.1 ha resolution thematic excess water maps derived from high-resolution satellite images, not only the open excess water surfaces could be detected and delineated, but also the vegetation in water and the highly saturated soil, which is very destructive to agricultural cultivation. During the pixel-based classification of satellite images taken by the sensors of the applied SPOT, Landsat and IRS-1C/1D LISS-III satellites, the determination of the sample areas might run into difficulties as the great number of the spectrally heterogeneous pixels might cause inaccuracy concerning the classification of the transitional areas.

In case of satellites revolving in a Sun-synchronous orbit, optical satellite images are taken at a well-determined point in time, however, in these spectral bands cloud cover frequently inhibits image-taking. Thus, the images of microwave imaging sensors (ENVISAT, MERIS, ASAR, RADARSAT and ERS) are effectively applicable for flood and excess water mapping, as well as in operative works (Csekő Á., 2003). However, by excess water maps based on radar data only the open water surfaces and the saturated soil areas could be delineated. Regarding the images of the year 2000, the radar data by themselves were limitedly suitable for high-resolution excess water mapping, however, they complete the data derived from the optical systems well.

Since the Landsat image database became accessible in 2009, it is possible to process satellite images taken from the year 1985, with using new, non-traditional methods different from the pixel-based classi-

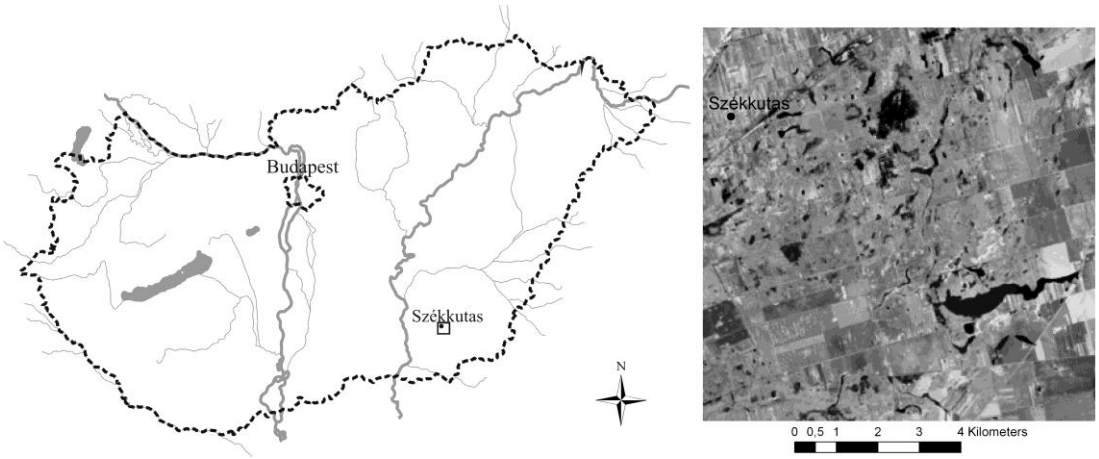

Fig. 1 The area under study

fication. These methods are mainly sub-pixel based classifications and they are applied principally on images taken in periods of extended excess water inundation, under clear weather conditions.

THE STUDY AREA

The area under study is situated in the south-eastern part of the Great Hungarian Plain, in the vicinity of the settlement Székkutas. Regarding land use, it is characterized by agricultural lands and protected areas belonging to the Körös-Maros National Park. The designated study area is 86 km^2 and is on the boundary of Csongrád and Békés counties. In terms of excess water hazard, it belongs to the 'medium hazard' category (Pálfai I. et al., 2004). The relief differences are minimal; the elevation values are between 81 m and 89 m.

DATA APPLIED AND THEIR PREPARATION FOR PROCESSING

During the survey, two years characterised by excess water inundation were chosen and one image taken in each year respectively have been analysed. Excess water inundation was considerable in the year 1986, while it was extreme in the year 2000 (Pálfai I., 2006). In these two years satellite images taken in early spring and early summer were selected, which were not disturbed by clouds. The time of the image-taking was as near to the period of the largest excess water inundation as possible. Data were downloaded from the web database (http://glovis.usgs.gov) of the U. S. Geological Survey (USGS). The area under study was also covered by the medium resolution images of the satellites Landsat-5 and Landsat-7, the catalogue numbers of which are 186/028 and 187/028. Thus, more images of the area became available and their time resolution was not only 16 days, but also 7 and 9 days.

A Landsat-5 TM image (row 187/coloumn 28) taken on 16th April 1986 and a Landsat-7 ETM+ image (row 186/coloumn 28) taken on 23rd April 2000 were selected, both of which were transformed to UTM projection system (WGS 84, zone 34).

Via atmospheric correction, the intensity values of the Landsat-5 TM and Landsat-7 ETM+ were transformed to reflectance values using an ERDAS IMAGINE model (Chavez P. S., 1996; Chander G.-Markham B. L., 2003).

To carry out accuracy estimation, the one-meter resolution colour infrared aerial photographs taken on 23rd April 2000 were available as reference data. In addition the digital database provided by the field survey of the Directorate for Environmental Protection and Water Management of Lower Tisza District (ATIKÖVIZIG) was also applied, which includes the patches of excess water in the inundated areas for the years characterized by inundation.

METHODS

Spectral mixture analysis

The significant advantages of the medium resolution (30 m) TM and ETM+ images of Landsat satellites revolving in a Sun-synchronous orbit are, that they are multispectral images covering vast areas (185*185 km) and they can be transformed with high accuracy to medium scale (approx. 1:100000) land cover maps by traditional pixel-based classification. However, their disadvantage is, that if the reflectance features of the area change on a greater scale in the space (the smallest elements, patches of the landscape pattern are smaller), than the spatial

resolution of the satellite image, numerous so-called spectrally mixed pixels can be found in the image. One of the basic problems of excess water mapping is that the open water surfaces might be relatively small in area, therefore these surfaces, as well as the soil surfaces in the transitional areas and the areas covered by vegetation are difficult to classify owing to the numerous spectrally mixed pixels. For the classification of the spectrally mixed pixels the so-called Spectral Mixture Analysis method was developed (Roberts et al., 1998).

The aim of Spectral Mixture Analysis (SMA) is to determine the spatial ratio of the spectrally homogeneous land cover types, the so-called *endmembers*, within a pixel. Each endmember specifies an unmixed, pure land cover type. The Linear Spectral Mixture Analysis (LSMA) is the improvement of the SMA method, by which the ratio of land cover types can be determined by using minimum two, in case of an LTM picture six, endmembers. In order to be able to solve the linear system of equations (1), the number of the endmembers has to be less than the number of the spectral bands of the image.

$$R_b = \sum_{i=1}^{N} f_i \cdot R_{i,b} + \varepsilon_b \tag{1}$$

R_b: the reflectance value of the image in band b;
N: the number of endmembers;
f_i: the ratio factor of endmember i;
R_{ib}: the reflectance value of the i^{th} endmember in band b;
ε_b: residual error.

The sum of the ratio factors of the endmembers equals 1 in every pixel and $f_i \geq 0$.

$$\sum_{k=1}^{n} f_{i,k} = 1 \tag{2}$$

The suitability of the model can be determined on the basis of the ε_b residual error or on the basis of the value of the root mean square error (RMSE) for each band of the image.

$$RMSE = \frac{\sqrt{\sum_{i=1}^{n} \varepsilon_i^2}}{n} \tag{3}$$

The endmembers are usually selected from the different bands of the satellite images or 2D scatter plots worked out from the bands (Rashed T. et al., 2001). By Principal Component Analysis (PCA), the endmembers are easier to determine, since it assembles almost 90 % of the data variance into the first two or three bands and reduces the correlation between the bands to a minimum (Smith M. O. et al., 1985). The other frequently applied transformation, which is also applied in this present research, is the minimum noise fraction (MNF) method. It consists of two main steps: (1) in the first step the noise fractions of the database are decorrelated and rescaled on the basis of an estimated noise covariance matrix and transformed data is provided, in which the noise has unit variance and there is no correlation between the bands; (2) in the second step a traditional PCA is carried out (Green A. A. et al., 1988).

The Pixel Purity Index (PPI), that selects the spectrally most pure (extreme) pixels from multispectral or hyperspectral images, was also applied to specify the endmembers. Employing iterative methods, the PPI creates N-dimensional spectral spaces on randomly chosen unit vectors. This procedure determines the extreme pixels (those that are at the end of the unit vector) in each projection, and records how many times the given pixel was specified as extreme. The value of each pixel in the resulting image is equal to this number (Broadman J. W. et al., 1994).

In the first step, MNF images were created for the Landsat TM image taken on 16th April 1986, which resulted in another 6 bands. The information content of the images is continuously decreasing after one another, thus the first three bands contain 89.5% of the total information content. The last bands predominantly contain only noise. The MNF images were used as input data for the PPI calculation, during which process the extreme pixels were defined by the algorithm after 1000 repetition.

On the basis of the first three MNF images and the resulting image of the PPI, three endmembers were defined for the linear spectral mixture: (1) the water surfaces, (2) the vegetation, and (3) the soil. These endmembers were pointed out in the spectral space formed by the first three MNF-bands and were detected at the margins and peaks of the 2D scatter plot.

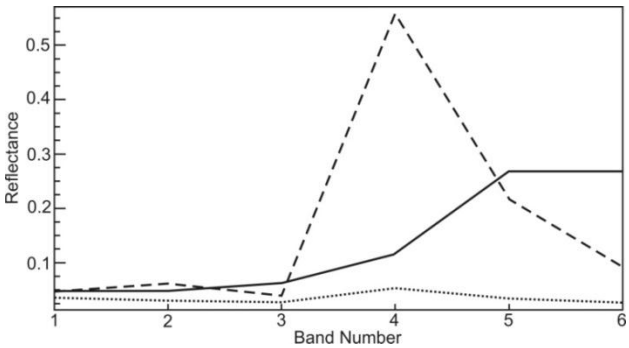

Fig. 2 The reflectance curves of soil, vegetation and water surfaces

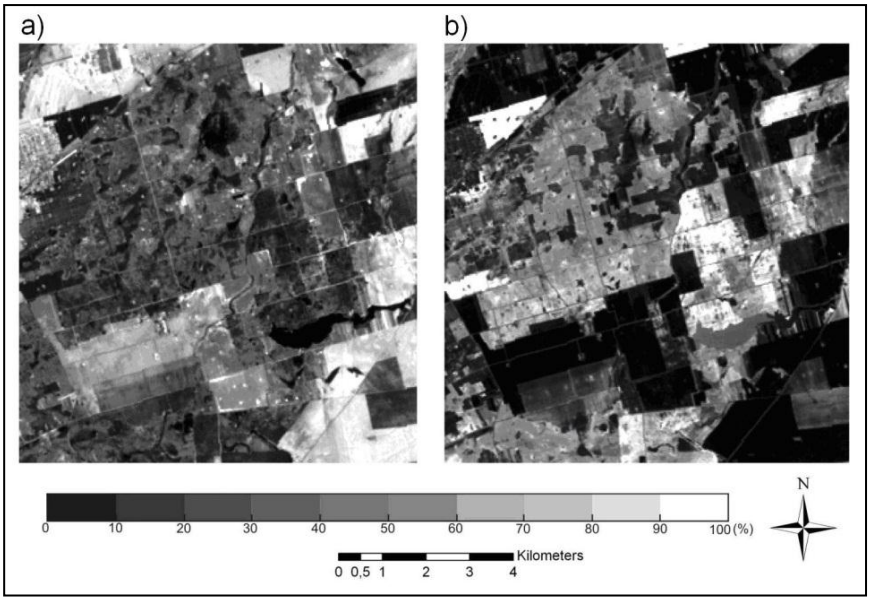

Fig.3 The ratio map of (a) the soil and (b) the vegetation based on the Landsat TM image taken on 16th April 1986.

DEFINING THE LAND COVER RATIO OF THE PIXELS

The outcomes of the LSMA are the maps showing the ratio of endmembers (soil, vegetation and water) within a pixel. The three maps represent the spatial distribution of the aforementioned land cover types for each pixel. The value of the pixels varies between 0 and 1. If the value equals 1, the ratio of a certain land cover type within the pixel is 100 % (*Fig. 3*).

On the gray-scale ratio map of the soil fractions (*Fig. 3a*), the open soil surfaces, are marked with light grey colour, where their ratio is 80-100%. The ratio of vegetation varies between 70 and 100 % on the arable lands, grasslands and pastures (*Fig. 3b*).

The open areas covered with excess water are marked with white and light grey colours on the gray-scale ratio map of water surfaces (*Fig. 4*) where the ratio of the water covered surface is about 70-100 % within a pixel. The Lake Fehér near to the settlement Kardoskút stretches along as a light grey patch on the south-eastern part of the area. Furthermore the excess water in abandoned riverbeds and on arable lands also has high fractional values on the ratio maps. The grey coloured territories are wet soils (saturated soils) and vegetation in water, where the ratio of surface water varies between 30 and 70 %.

Similarly, maps representing the land cover ratio within the pixels were created based on the Landsat ETM+ images taken on 23rd April 2000 (*Fig. 5*). By the analysis of the ratio maps of the water surfaces, the extent of inundation at the two dates can be examined, the total area covered with excess water can be determined and the spatial pattern of the patches of excess water can be compared.

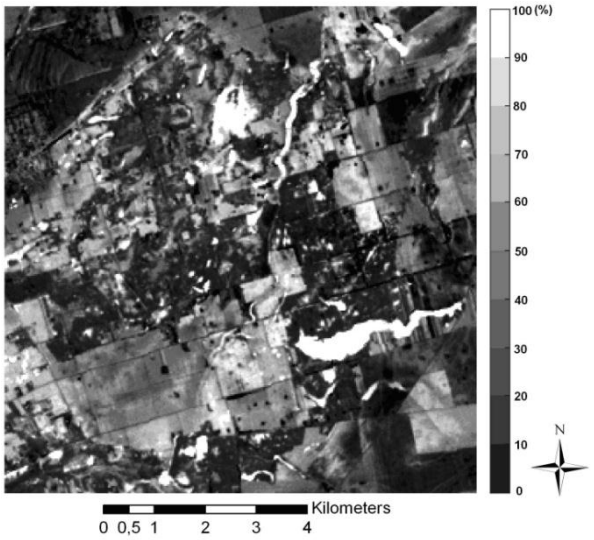

Fig. 4 The ratio map of water surfaces based on the Landsat TM image taken on 16th April 1986.

5. RESULTS AND ACCURACY ESTIMATION

The classification of land cover ratio maps by using supervised classification

A supervised classification was carried out on the 3-band image (1: soil, 2: vegetation, 3: water ratio map), which was the result of the LSMA. Based on the three endmembers seven classes were created. Three of the

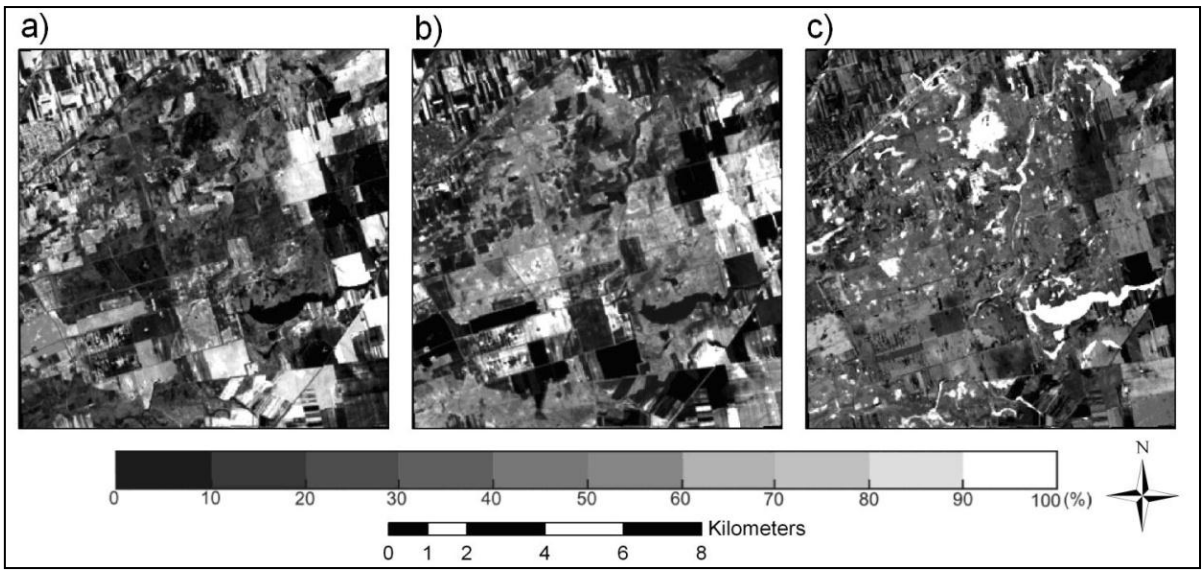

Fig. 5 The ratio maps of land cover types based on the Landsat ETM+ image taken on 23rd April 2000. a) soil, b) vegetation, c) water surfaces

seven classes mainly contain one land cover type, another three classes contain two land cover types and there is one more class that includes all the three land cover types nearly in equal proportion.

When the study area was selected, the upper and lower limits of soil, vegetation and open water surfaces were defined. On the basis of this, the following seven classes were defined: (1) open water surfaces, (2) vegetation, (3) open soil surfaces, (4) saturated soil, (5) vegetation in water, (6) soils covered with vegetation and (7) other. The classes are represented in a triangle diagram (*Fig. 6*). During the supervised classification the parallelepiped decision rule was applied. In case of overlapped areas, the certain pixels were assigned to one of the classes by using the minimum distance method.

Similarly, the supervised classification was carried out on the Landsat ETM+ image taken on 23rd April 2000, which resulted in a thematic map with the same 7 classes. The water covered surfaces marked with black colour, the saturated soils and the wet soils can be easily distinguished on the map (*Fig. 7-8*).

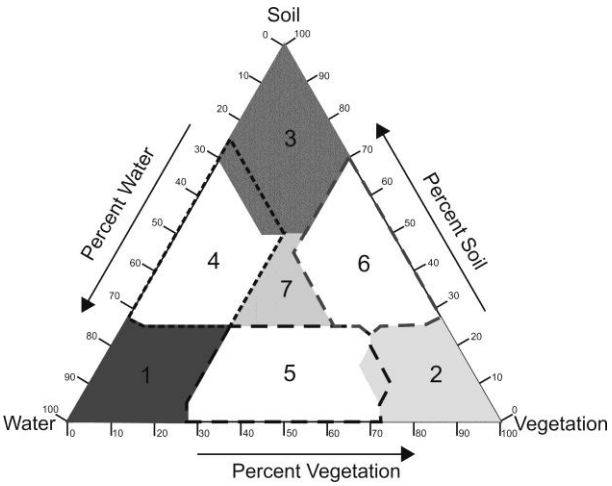

Fig.6 The triangle diagram representing the seven land cover types

	Lower_1	Upper_1	Lower_2	Upper_2	Lower_3	Upper_3	Lower_4	Upper_4
Soil	0%	27.5%	0%	27.5%	50%	100%	25%	75%
Vegetation	0%	27.5%	60%	100%	0%	30%	0%	25%
Water	50%	100%	0%	27.5%	0%	30%	25%	72.5%

	Lower_5	Upper_5	Lower_6	Upper_6	Lower_7	Upper_7
Soil	0%	25%	25%	75%	25%	50%
Vegetation	27.5%	75%	30%	70%	25%	50%
Water	20%	70%	0%	25%	25%	50%

Table 1 The upper and lower limits of the land cover types according to the endmembers

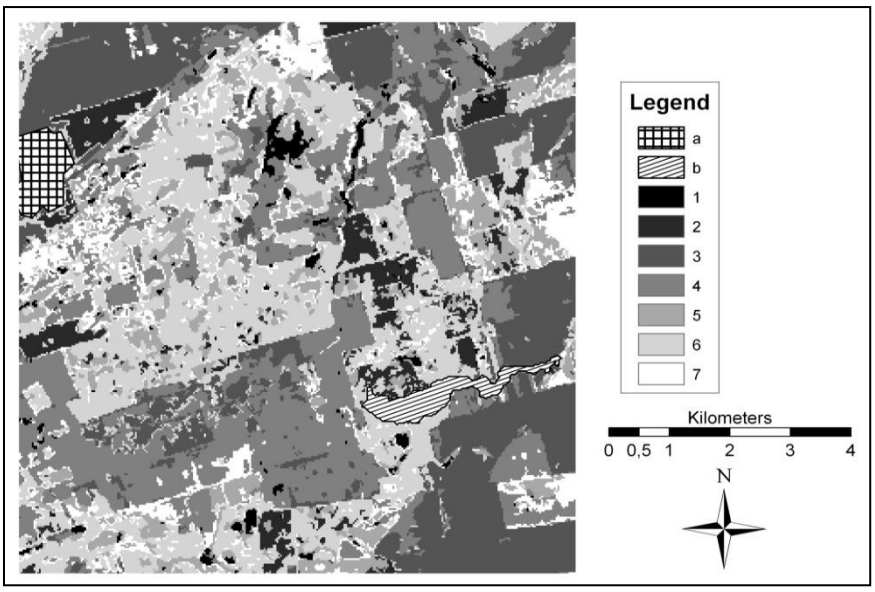

Fig. 7 Thematic map based on the endmember ratios of the Landsat TM satellite image taken on 16th .April 1986.
(a) Székkutas, (b) Lake Fehér, (1) open water surfaces, (2) vegetation, (3) open soil surfaces, (4) saturated soil(5) vegetation in water (6) soils covered with vegetation, (7) other

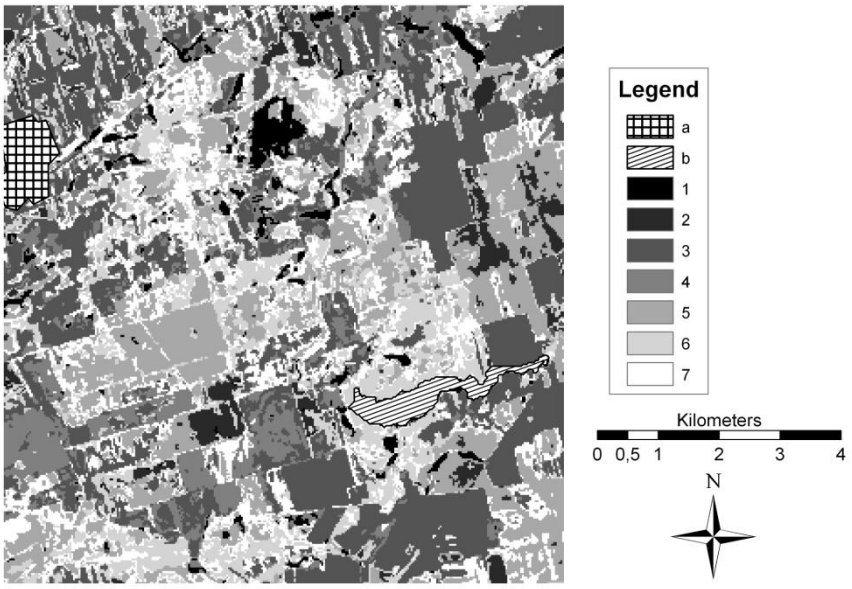

Fig. 8 Thematic map based on the endmember ratios of the Landsat ETM+ satellite image taken on 23rd April 2000.
(a) Székkutas, (b) Lake Fehér, (1) open water surfaces, (2) vegetation, (3) open soil surfaces, (4) saturated soil, (5) vegetation in water, (6) soils covered with vegetation, (7) other

By comparing the open water surface classes of the two examined dates, the location of the patches of excess water and the total extent of excess water coverage can be defined (*Fig 9*). It can be concluded that the patches of excess water occupy similar locations on the two images, however, there is a difference regarding their extension. The total surface of the patches was 1.52 km^2 in 1986, a year characterised by considerable excess water inundation and it was 2.63 km^2 in 2000, a year characterised by extreme excess water inundation.

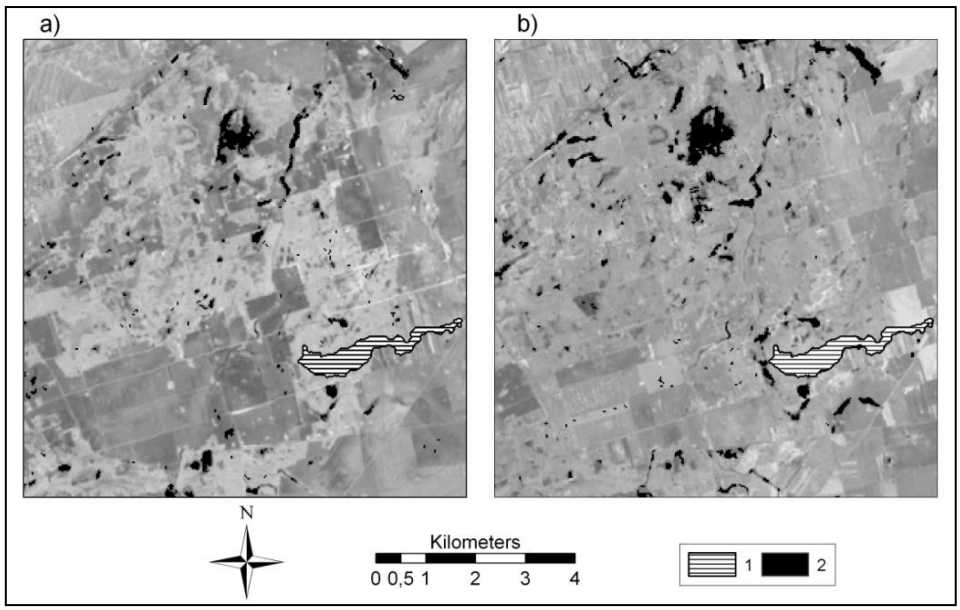

Fig. 9 The comparison of the patches of excess water on the images taken on 16th April 1986 (a) and 23rd April 2000 (b) (1) Lake Fehér (2) open water patches

Accuracy estimation

In the first step the results of the classification were compared with the data produced by the field surveys of the Directorate for Environmental Protection and Water Management of Lower-Tisza District (ATIKÖVIZIG). Our classes of the open water surfaces, the saturated soil and the inundated vegetation were compared with the excess water polygons as references (*Fig. 10*). On the basis of the comparison it can be concluded that due to their smaller scale, the field surveys are less detailed. There are some patches of excess water on the satellite images that can be detected without any image processing method, but they are in areas that are difficult to approach, hard to walk round, thus these patches are missing from the results of the field surveys. The classification based on satellite images is also favourable, as this way the saturated soils can be differentiated from the vegetation in water, while field surveys do not produce such descriptive data.

Other available data that can be used as reference to estimate the accuracy of the classification are the aerial photographs taken of the Tiszántúl, in the vicinity of Székkutas on 23rd March 2000 (*Fig. 11*). Although the photographs with 1 m geometrical resolution are appropriate for the visual determination of the land cover types, the precise separation and classification of certain water surfaces on the 3 band photos are hard to carry out with automatic image processing methods.

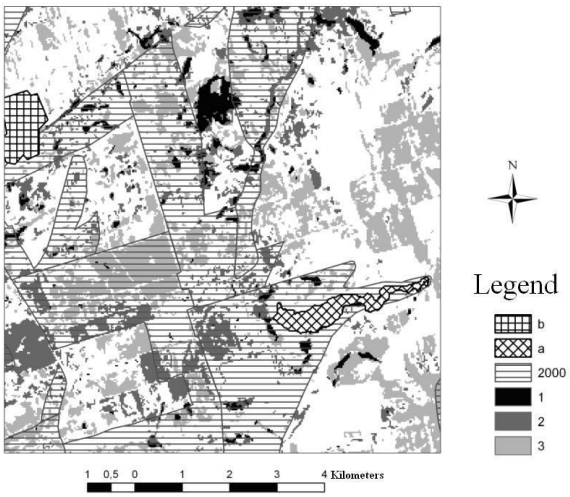

Fig. 10 The comparison of the patches of excess water of the three classes of the thematic layer and the field survey (a) Székkutas, (b) Lake Fehér, (1) open water surfaces, (2) saturated soils, (3) vegetation in water

In order to prove the importance of the SMA-classification, the created thematic layer was compared with the results of a traditional pixel-based classification. ISODATA classification was carried out on the Landsat ETM+ 6 band image taken on 23rd April 2000 (*Fig. 12*), during which process 7 output classes were set. Subsequently the 7 land cover classes of the thematic layer were compared with the adequate classes of the ISODATA clustering by using the cross-tabulation method (*Table 2*).

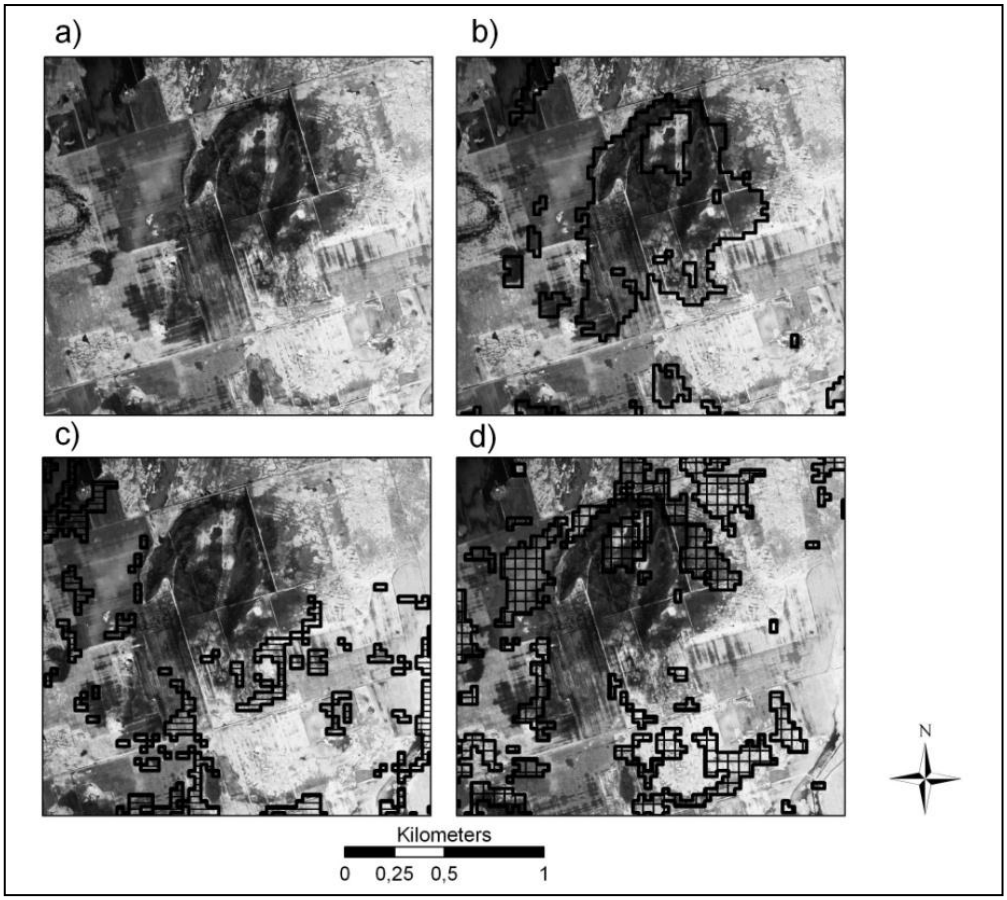

Fig. 11 The aerial photograph (a) and the polygons of the certain classes: (b) open water surface, (c) wet (saturated) soil (d) vegetation in water

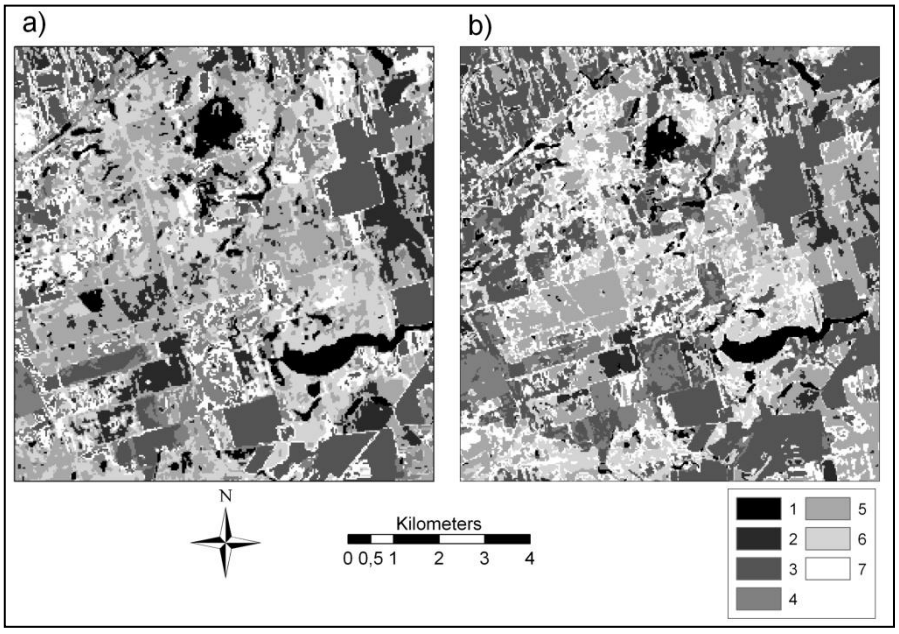

Fig. 12 Images based on the ISODATA classification (a) and the SMA-image classification (b)
(1) open water surfaces, (2) vegetation, (3) open soil surfaces, (4) saturated soil, (5) vegetation in water, (6) soil covered with vegetation, (7) other

		ISODATA classes						
		1	2	3	4	5	6	7
SMA- image classes	Open water surfaces	67.3%	0.5%	-	0.4%	0.1%	-	-
	Vegetation	-	41.8%	-	-	0.1%	-	-
	Open soil surfaces	0.1%	0.2%	92.5%	7.2%	0.3%	3.2%	92.0%
	Saturated soil	9.6%	-	6.6%	59.6%	-	1.4%	4.4%
	Inundated vegetation	22.4%	54.0%	-	3.0%	66.0%	0.5%	-
	Soil covered with vegetation	-	3.2%	0.8%	0.3%	10.8%	53.0%	3.1%
	Other	0.7%	0.1%	0.1%	29.5%	22.7%	41.9%	0.5%

Table 2 The comparison of the ISODATA classification and the SMA-image classification using the cross-tabulation method

On the basis of these, the open water surface class of the ISODATA classification shows a 67.3% concordance with the water surfaces gained following the SMA classification. Furthermore, 22.4% and the 9.6% of the open water surface class of the ISODATA classification have been classified as vegetation in water and as saturated soils, respectively. The class of vegetation shows a 41.8% concordance with the SMA classification, however, 54% have been classified as vegetation in water. The soil surfaces show 92.5% concordance. There has been a 59.6% and 66% concordance regarding the wet (saturated) soil and the vegetation in water, respectively.

6. CONCLUSIONS

On the basis of our research it can be concluded that by using a sub-pixel based classification, the medium resolution satellite images are suitable for mapping excess water. The satellite images being available since the mid-1980s provide an opportunity to create excess water hazard maps. The classes of the thematic maps created by the linear spectral mixture analysis are able to provide more detailed results than the traditional pixel-based classifications. The excess water patches of the earlier field surveys are precisely identifiable and by the help of the applied methods the creation of these maps can be made automatic.

Acknowledgement

The present research was financially supported by the Economic Operative Program (GOP)

References

Boardman J. W. 1994. Geometric mixture analysis of imaging spectrometry data, *Proc. Int. Geoscience and Remote Sensing Symp*., vol. 4, pp. 2369-2371

Chander G. – Markham B. L. Revised Landsat-5 TM Radiometric Calibration Procedures, and Post-Calibration Dynamic Ranges, *IEEE Transactions on Geoscience and Remote Sensing* 41/11 (2003): 2674–2677

Chavez P.S. jr. Image-based atmospheric corrections – Revisited and Improved. *Photogrammetric Engineering and Remote Sensing* 62/9 (1996): 1025-1036

Csekő Á. 2003. Árvíz- és belvízfelmérés radar felvételekkel [Flood- and excess water mapping based on radar images] *Geodézia és Kartográfia,* 55/2 (2003): 16-22

Csornai G. – Lelkes M. – Nádor G. – Wirnhardt Cs. Operatív árvíz- és belvízmonitoring távérzékeléssel. [Operative monitoring of floods and excess water based on remote sensing] *Geodézia és Kartográfia* 52/5 (2000): 6-12

Green A. A. – Berman M. – Switzer P. – Craig M. D. A transformation for ordering multispectral data in terms of image quality with implications for noise removal. *IEEE Transactions on Geoscience and Remote Sensing* 26 (1988): 65-74

Licskó B. 2009 Belvizek légi felmérésének tapasztalatai, [The experiences of the aerial photography of excess water] Magyar Hidrológiai Társaság XXVII. Országos Vándorgyűlés, Baja 2009.

http://www.hidrologia.hu/vandorgyules/27/dolgozatok/4szekcio.html

Pálfai I. Belvízgyakoriság és belvízkárok Magyarországon [The frequency of excess water events and the damages caused in Hungary]. *Hidrológiai Közlöny* 86/5 (2006): 25-26

Pálfai I. – Bozán Cs. – Herceg Á. – Kozák P. – Körösparti J. – Kuti L. – Pásztor L. 2004. Komplex Belvíz-veszélyeztetettségi Mutató (KBM) és Csongrád megye ez alapján szerkesztett belvíz-veszélyeztetettségi térképe, [Mapping of excess water hazard in Csongrád county based on the Complex Excess Water Hazard Index] II. Magyar Földrajzi Konferencia. Szeged, 2004. szeptember 2-4. ISBN 963 482 687 3

Rashed T. – Weeks J. R. – Gallada M. S. Revealing the anatomy of cities through spectral mixture analysis of multispectral satellite imagery: a case study of the greater Cairo region, *Egypt. Geocarto International* 16/4 (2001): 5-15

Rakonczai J. – Mucsi L. – Szatmári J. – Kovács F. – Csató Sz. 2001. A belvizes területek elhatárolásának módszertani lehetőségei. [Methodological possibilities for mapping excess water areas] In: A Magyar Földrajzi Konferencia tudományos közleményei CD. ISBN 9634825443. Szeged

Roberts D. A. − Gardner M. − Church R. − Ustin S. − Scheer G. − Green R. O. Mapping chaparral in the Santa Monica Mountains using multiple endmember spectral mixture models, *Remote Sensing of Environment* 65 (1998): 267–279

Smith M. O. – Johnson P. E. – Adams J. J. 1985. Quantitative determination of mineral types and abundances from reflectance spectra using principal components analysis, *Journal of Geophysical Research* **90.** C797–C804